Electronic Supplementary Material (ESI) for RSC Advances.

Supporting Information

One-Step Hydrothermal Synthesis of a Ni_3S_2-$FeMoO_4$ Nanowire-Nanosheet Heterostructure Array for Synergistically Boosted Oxygen Evolution Reaction

Han Chen,[#ab] *Jing Zhang,*[#bc] *Rui Wan,*[bc] *Xiang Zhang,*[bc] *Qijun Pan,*[bc] *Mingtao Li*[*d] *and Bin Chen*[*bc]

[a] Institutes of Physical Science and Information Technology, Anhui University, Hefei 230601, P. R. China

[b] Key Laboratory of Materials Physics and Anhui Key Laboratory of Nanomaterials and Nanotechnology, Institute of Solid State Physics, HFIPS, Chinese Academy of Sciences, Hefei 230031, China

[c] University of Science and Technology of China, 96 Jinzhai Road, Hefei, Anhui 230026, P. R. China

[d] School of Mechanical and Resource Engineering, Wuzhou University, Wuzhou 543002, China

[#] These authors contributed equally to this work

Experimental section

Chemicals and reagents: Ammonium molybdate tetrahydrate ($(NH_4)_6Mo_7O_{24}\cdot4H_2O$, purity ≥ 99.0%), thiourea (CH_4N_2S, purity ≥ 99.0%), and citric acid monohydrate ($C_6H_8O_7\cdot H_2O$, purity ≥ 99.8%) were acquired from Sinopharm Chemical Reagent Co., Ltd. Potassium hydroxide (KOH, 85%) was procured from Guangdong Guanghua Sci-Tech Co., Ltd. Deionized (DI) water was employed for all solution preparations. The commercial Ni-Fe foam (NFF, the atom ratio of Ni: Fe is 6: 4) and Ni foam (NF) were obtained from SuZhou Christie de Foam Metal Company. All the chemicals were employed without any further purification processes.

Treatment of NFF and NF: The NFF and NF were cleaned by the sonication in acetone, ethanol, and DI water for 30 min, respectively. Then, the NFF and NF were dried in a vacuum oven at 60 °C before synthesis.

Preparation of Ni_3S_2-$FeMoO_4$/NFF and NiMo-OS/NF: To prepare the Ni_3S_2-$FeMoO_4$/NFF, 60 mg $(NH_4)_6Mo_7O_{24}\cdot4H_2O$, 60 mg CH_4N_2S, and 15 mg $C_6H_8O_7\cdot H_2O$ were added into 30 mL DI water under stirring for 5 min. Subsequently, the homogeneous solution and the cleaned NFF were transferred to a 50 mL stainless autoclave with Teflon liner and sealed, followed by heat treatment at 200 °C for 10 h. After cooling to room temperature, the products were rinsed three times with DI water and dried at 60 °C to obtain Ni_3S_2-$FeMoO_4$/NFF electrode. The contrast electrodes with the same stoichiometry were prepared for 4 and 16 h, respectively. The contrast sample of NiMo-OS/NF was prepared by the same hydrothermal process except for using NF instead of the NFF. The NF was immersed in the same precursor solution as mentioned above and followed by heat treatment at 200 °C for 10 h.

Preparation of IrO_2/NF: For comparison, 30 mg IrO_2 and 50 μL Nafion solution were dispersed in 1.0 mL ethanol and 0.45 mL DI water by sonication for 1 h. Then 60 μL of the homogeneous suspension was dropped onto the treated NFF, where the total load mass of IrO_2 is approximately 1.2 mg cm^{-2}.

Characterization technology: X-ray Diffraction (XRD, Rigaku SmartLab system) with Cu Kα radiation was aim to analyze crystal phase of the synthesized products. The morphologies of these electrocatalysts were examined by using Scanning Electron Microscopy (SEM, Hitachi SU8020) and Transmission Electron Microscopy (TEM, FEI Tecnai G2 F20). X-ray Photoelectron Spectroscopy (XPS, Thermo Scientific TM K-Alpha TM+ spectrometer equipped with a monochromatic Al K_α X-ray source) was carried out to investigate the valence states and chemical composition of the elements. Additionally, a Renishaw inVia confocal microscopic Raman spectrometer, fitted with a 50× objective lens, was employed to explore the chemical and molecular structures of the samples.

Electrochemical experiments: Electrochemical experiments were performed by CHI760E electrochemical workstation and ZAHNER PP212 electrochemical workstation, equipped with a standard three-electrode system. All potential measurements were corrected with iR compensation resistance (90 %), referenced to the reversible hydrogen electrode (RHE) scale. In these experiments, the as-prepared electrodes served as the working electrode, the Hg/HgO electrode and Pt mesh electrode were used as the reference and counter electrodes, respectively. Linear sweep voltammetry (LSV) curves were recorded at a scan rate of 5 mV s^{-1}. Electrochemical impedance spectroscopy (EIS) tests were conducted over a frequency range of 0.01 Hz to 10 MHz at an overpotential of 294 mV. The double-layer charging capacitance (C_{dl}) was determined from cyclic voltammetry (CV) curves in a non-Faradaic region,using different scan rates of 20, 40, 60, 80, and 100 mV s^{-1}. The electrochemical active surface area (ECSA) was obtained from the formula: ECSA=C_{dl}/C_s (C_s=40 μF). Chronoamperometry were carried out to monitor the operation durability of electrodes.

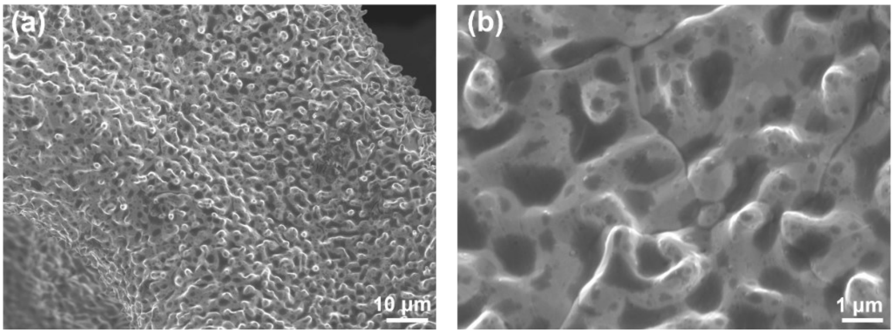

Figure S1. SEM images of the pristine Ni-Fe foam.

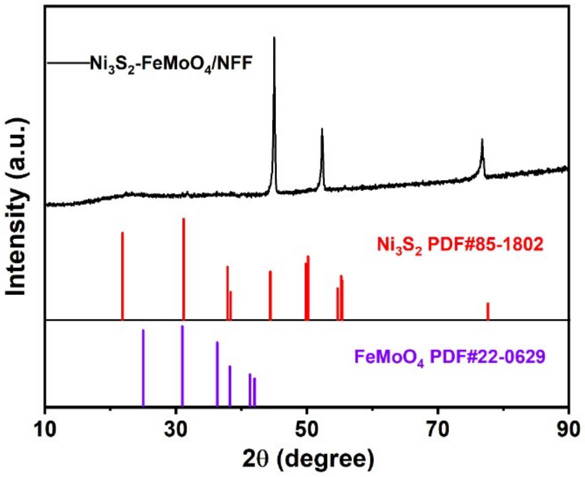

Figure S2. XRD pattern of the Ni_3S_2-$FeMoO_4$/NFF electrode.

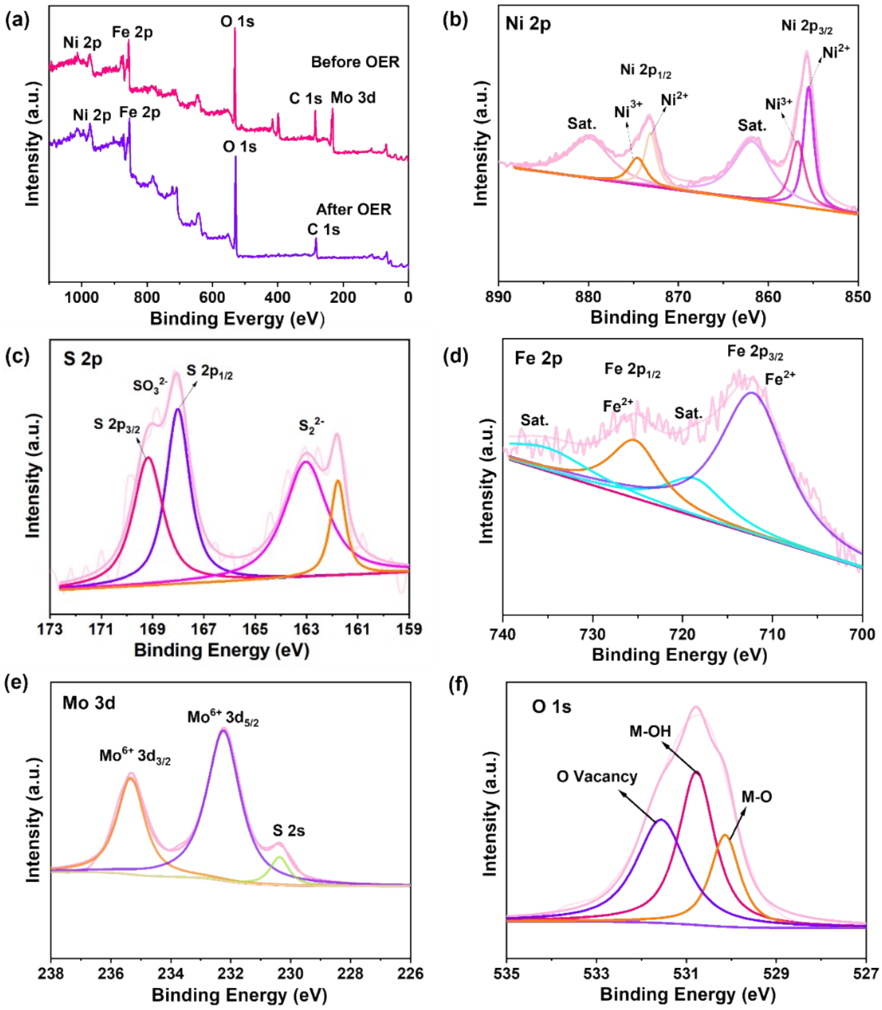

Figure S3. (a) The XPS full spectra of the Ni_3S_2-$FeMoO_4$ electrode before and after the OER test. (b-f) High resolution XPS spectra of Ni 2p, S 2p, Fe 2p, Mo 3d, and O 1s for the Ni_3S_2-$FeMoO_4$ electrode before the OER test.

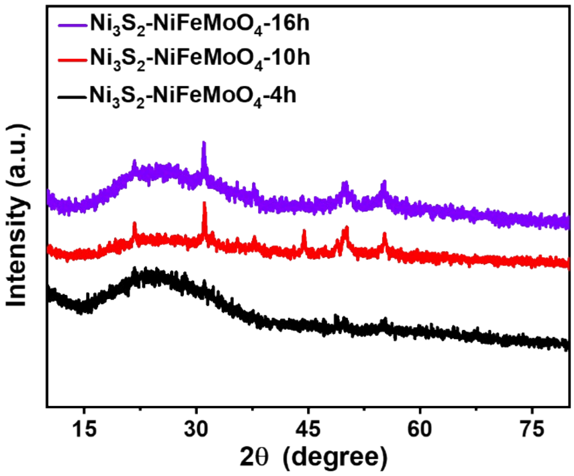

Figure S4. XRD patterns of the Ni_3S_2-$FeMoO_4$ electrodes synthesized with different hydrothermal times of 4 h, 10 h, and 16 h.

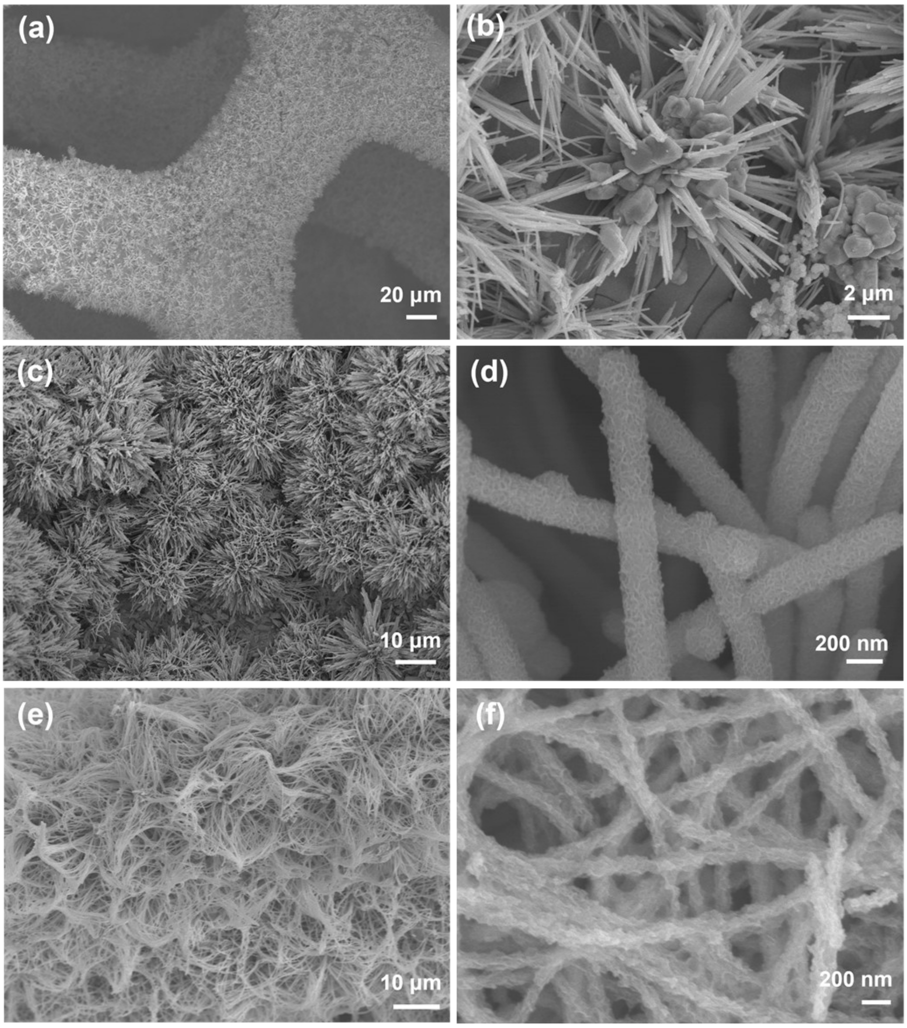

Figure S5. SEM images of the Ni_3S_2-$FeMoO_4$ electrodes synthesized with different hydrothermal times of (a, b) 4 h, (c, d) 10 h, and (e, f) 16 h.

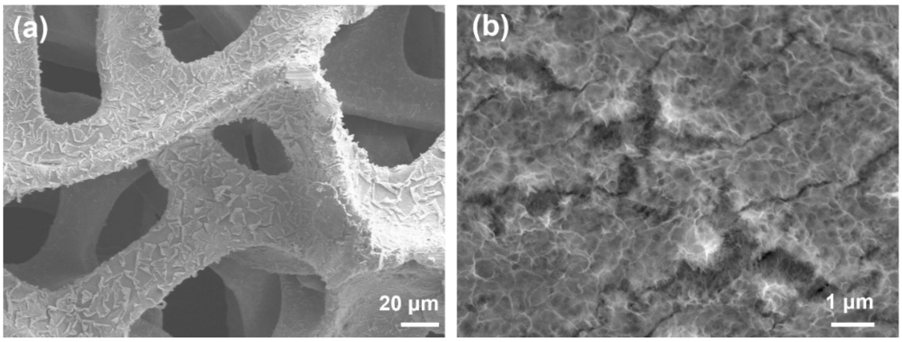

Figure S6. SEM images of the NiMo-OS/NF electrode synthesized on Ni foam at 200 ℃ for 10 h.

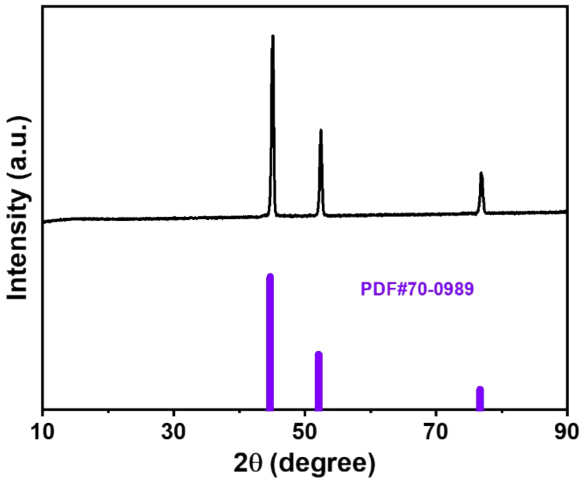

Figure S7. XRD pattern of the NiMo-OS/NF synthesized on Ni foam at 200 °C for 10h.

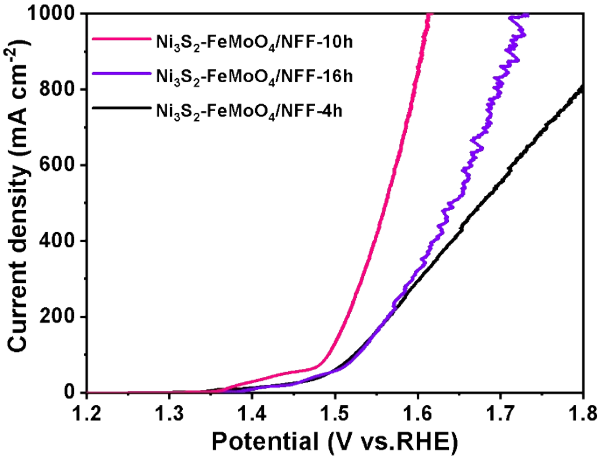

Figure S8. LSV curves of Ni_3S_2-$FeMoO_4$/NFF synthesized at 200 °C with different hydrothermal times of 4 h, 10 h, and 16 h.

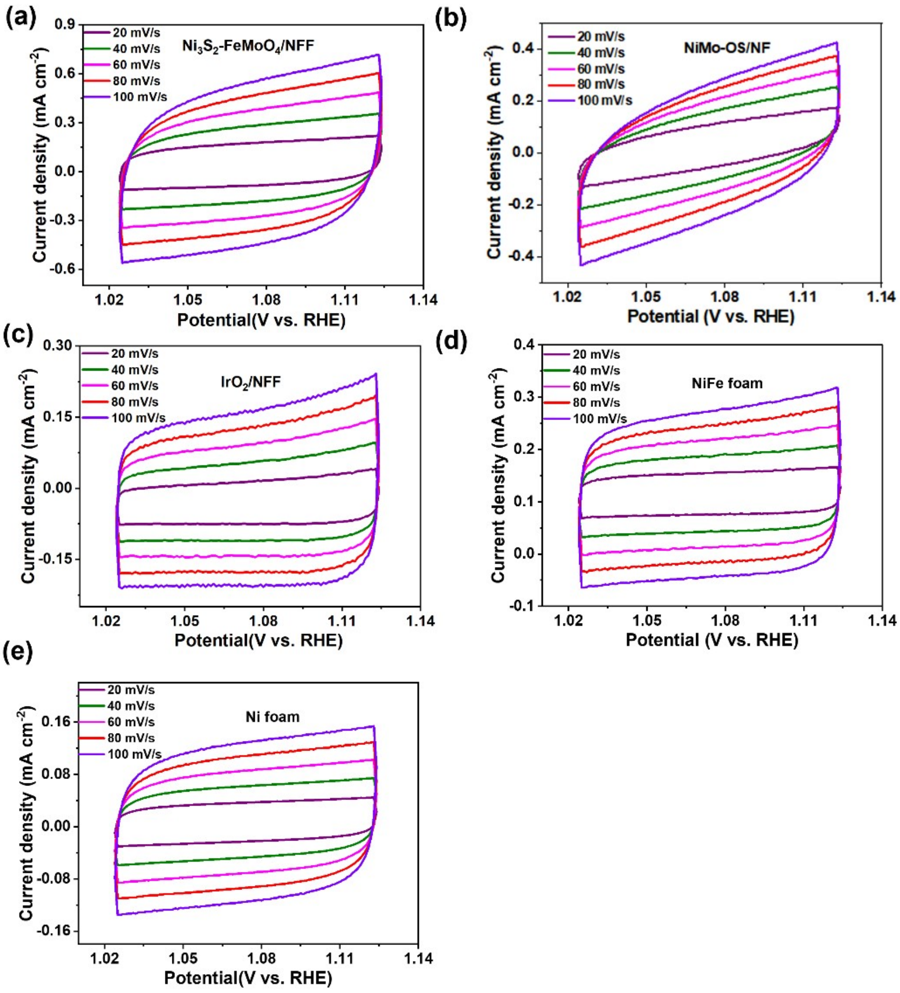

Figure S9. Cyclic voltammograms of (a) Ni_3S_2-$FeMoO_4$/NFF, (b) NiMo-OS/NF, (c) IrO_2/NF, (d) NiFe Foam, and (e) Ni Foam.

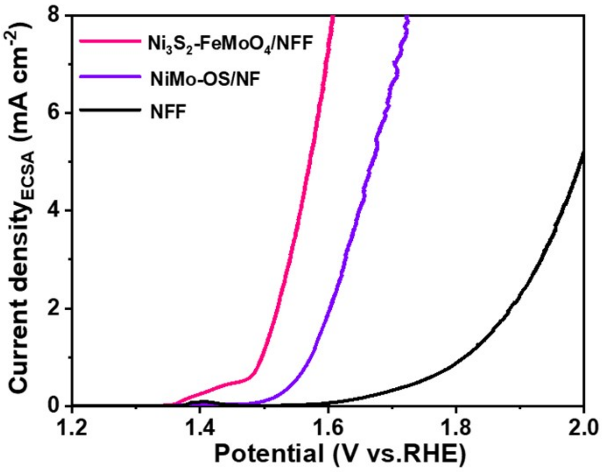

Figure S10. LSV curves of different electrodes of Ni_3S_2-$FeMoO_4$/NFF, NiMo-OS/NF, and NiFe foam normalized by ECSA in 1.0 M KOH solution.

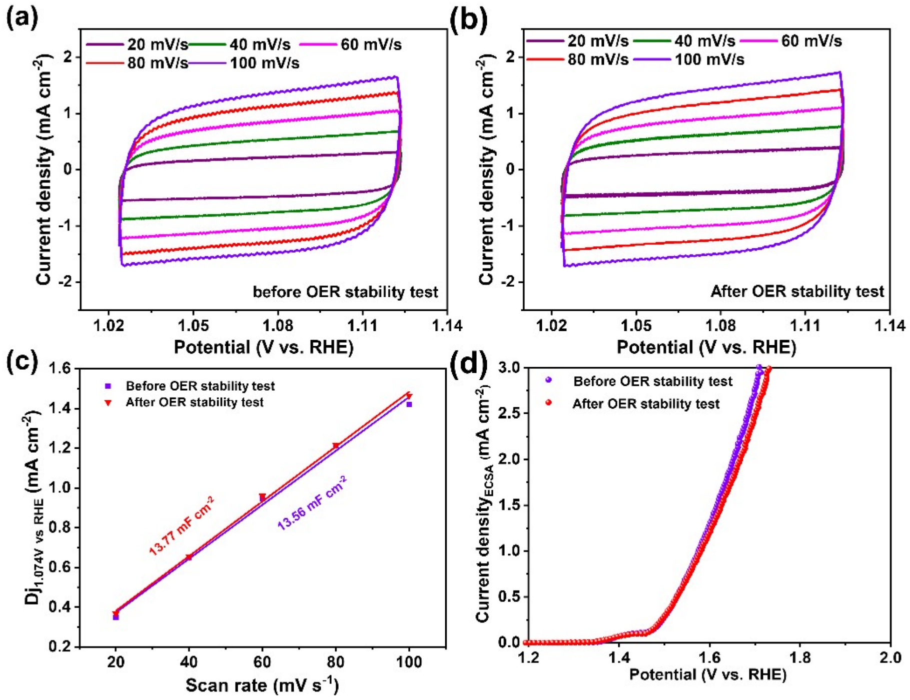

Figure S11. Cyclic voltammograms of Ni_3S_2-$FeMoO_4$/NFF (a) before OER stability test and (b) atter OER stability test. (c) Double-layer capacitances Ni_3S_2-$FeMoO_4$/NFF before and after OER stability test. (d) LSV curves of Ni_3S_2-$FeMoO_4$/NFF normalized by ECSA before and after OER stability test.

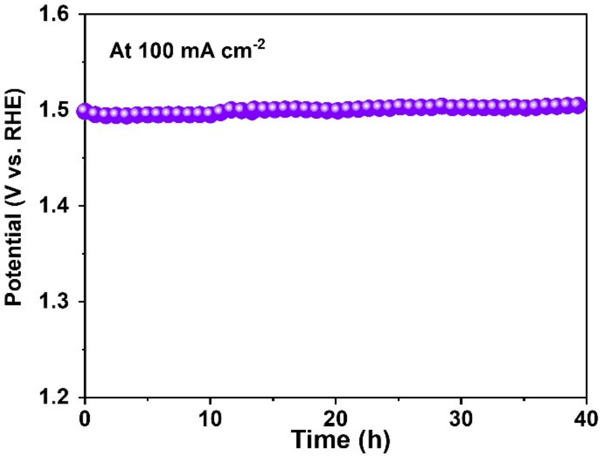

Figure S12. Chronopotentiometry curve of Ni_3S_2-$FeMoO_4$/NFF at 100 mA cm^{-2},

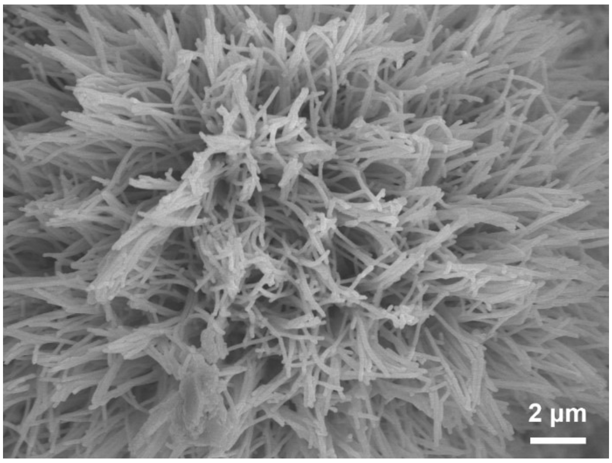

Figure S13. SEM image of Ni_3S_2-$FeMoO_4$/NFF electrode after OER test.

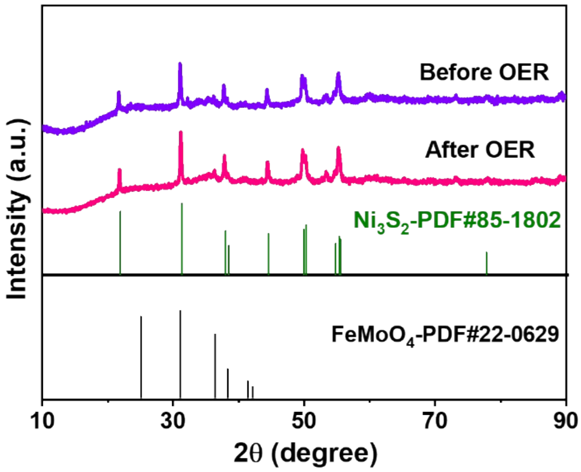

Figure S14. XRD patterns of the Ni_3S_2-$FeMoO_4$/NFF before and after OER stability test.

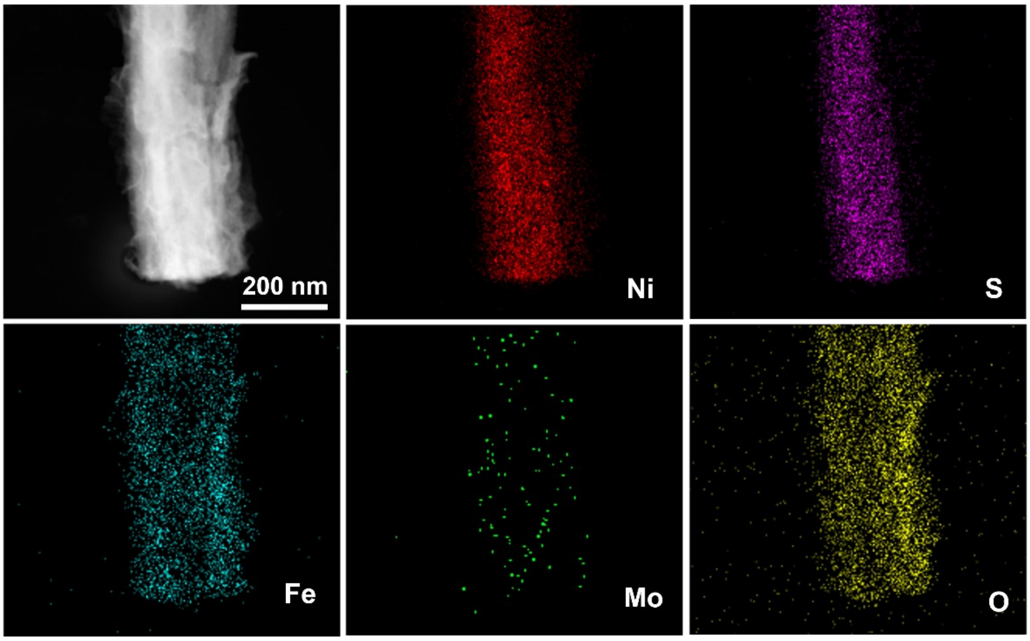

Figure S15. HAADF-STEM image of the Ni_3S_2-$FeMoO_4$/NFF after OER test and the corresponding mapping elements of Ni, S, Fe, Mo, and O.

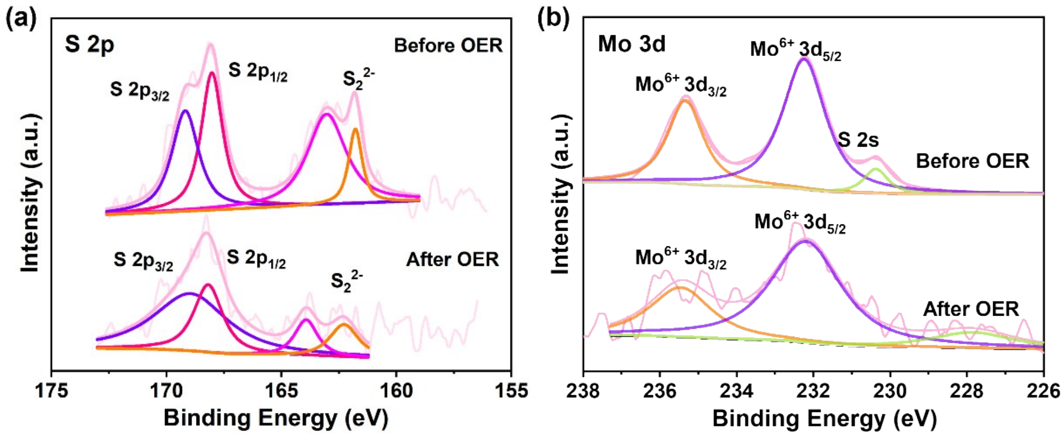

Figure S16. XPS spectra of the Ni_3S_2-$FeMoO_4$ electrode before and after OER test. (a) S 2p and (b) Mo 3d.

Table S1. The compositional ratio of Ni_3S_2-$FeMoO_4$/NFF determined by TEM/EDX before and after OER stability test.

Elements	Before OER stability	After OER stability
Ni	11.5	26.5
Fe	2.8	7.2
Mo	52.0	3.4
S	5.8	25.8
O	27.9	37.1